Surface Rupture of the November 2002 M7.9 Denali Fault Earthquake, Alaska, and Comparison to Other Strike-Slip Ruptures

Peter J. Haeussler, David P. Schwartz, Timothy E. Dawson, Heidi D. Stenner, James J. Lienkaemper, Francesco Cinti, Paola Montone, Brian Sherrod, and Patricia Craw

Corresponding (first) author: Peter J. Haeussler

Mailing address: U.S. Geological Survey

4200 University Drive

Anchorage, AK 99508

Phone: 907-785-7447

Fax: 907-785-7401

E-mail address: pheuslr@usgs.gov

Surface Rupture of the November 2002 M7.9 Denali Fault Earthquake, Alaska, and Comparison to Other Strike-Slip Ruptures

Peter J. Haeussler,[a] David P. Schwartz,[b] Timothy E. Dawson,[b] Heidi D. Stenner,[b] James J. Lienkaemper,[b] Francesca Cinti,[c] Paola Montone,[c] Brian Sherrod,[d] and Patricia Craw [e]

On November 3, 2002, a moment-magnitude (Mw) 7.9 earthquake produced 340 km of surface rupture on the Denali fault and two related faults in central Alaska. The rupture, which proceeded from west to east, began with a 40-km-long break on a previously unknown thrust fault. Estimates of surface slip on this thrust were 3-6 m. Next came the principal surface break, along 220 km of the Denali fault. There, right-lateral offset averaged almost 5 m and increased eastward to a maximum of nearly 9 m. Finally, slip turned southeastward onto the Totschunda fault, where dextral offsets up to 3 m continued for another 70 km. This three-part rupture ranks among the longest documented strike-slip events of the past two centuries. The surface-slip distribution supports and clarifies models of seismological and geodetic data that indicated initial thrusting followed by right-lateral strike slip, with the largest moment release near the east end of the Denali fault. The Denali fault ruptured beneath the Trans-Alaska oil pipeline. The pipeline withstood almost 6 m of lateral offset, because engineers designed it to survive such offsets based on pre-construction geological studies. The Denali fault earthquake was typical of large-magnitude earthquakes on major intracontinental strike-slip faults, in the length of the rupture, the multiple fault strands that ruptured, and the variable slip along strike.

[a] U.S. Geological Survey, 4200 University Dr., Anchorage, AK 99508
[b] U.S. Geological Survey, 345 Middlefield Rd., Menlo Park, CA 94025
[c] Istituto Nazionale di Geofisica e Vulcanologia, Via di Vigna Murata 605, 00143 Roma, Italy
[d] U.S. Geological Survey, University of Washington, Box 351310, Seattle, WA 98195
[e] Division of Geological and Geophysical Surveys, 345 College Road, Fairbanks, AK 99709

INTRODUCTION

The moment magnitude M_w7.9 Denali fault earthquake (Eberhart-Phillips et al., 2003) on 3 November 2002 was the largest strike-slip earthquake in North America in almost 150 years. The Denali fault earthquake ruptured beneath the Trans-Alaska Pipeline System (TAPS), in the first real test of a structure designed to allow fault offset. The pipeline, which transports about a million barrels of oil per day, performed according to design. It did not spill oil because pre-construction geologic and geotechnical studies correctly anticipated the consequences of an earthquake similar to the one of 3 November 2002 (Woodward-Lundgren Associates, 1974). This paper provides an overview of the surface faulting and slip distribution during the 2002 earthquake and compares this rupture to other large-magnitude strike-slip ruptures.

The earthquake occurred on a system of active intracontinental faults that accommodate a fraction of the oblique collision of the Yakutat terrane into the southern Alaska margin (Fig. 1). The collision is driven by northwest-dipping subduction at nearly 5 m per century along the Aleutian megathrust. Great earthquakes (M $\geq$ 8) in the 20th century, including the 1964 M9.2 earthquake, resulted from slip along the megathrust (Plafker, 1969). North and west of the Yakutat terrane collision zone, active crustal thrust and strike-slip faults accommodate westward escape of part of southern Alaska, shown by arrows on Figure 1 (Lahr and Plafker, 1980; Plafker et al.,1994; Haeussler et al., 2000). The Denali and Totschunda faults (St. Amand, 1957; Grantz, 1966; Richter and Matson, 1971) are the principal elements in an intracontinental dextral strike-slip fault system that curves across Alaska and western Canada and passes through the Alaska Range (Fig. 1). Only the Totschunda fault and segments of the Denali fault in the central and eastern Alaska Range have demonstrable pre-2002 active strike-slip displacement (Richter and Matson, 1971; Plafker et al., 1977, 1994).

The 3 November 2002 M7.9 earthquake was preceded by a M6.7 event on 23 October, 2002, which occurred ~22 km west of the M7.9 epicenter. The October earthquake, which is now considered to be a foreshock, occurred on the Denali fault trace, had aftershocks along the fault trace, and had a right-lateral focal mechanism (Alaska Earthquake Information Center (AEIC)). Wright et al. (2003) find excellent fit to Radarsat-1 interferograms using 1 m of offset during the earthquake. We overflew the epicentral region of the M6.7 event in a fixed wing aircraft on the day of the earthquake. The ground was snow covered, however, we saw no evidence of surface rupture.

DESCRIPTION OF SURFACE RUPTURE

The 3 November 2002 rupture progressed along three faults. From west to east, these are the Susitna Glacier, Denali, and Totschunda faults (Fig. 2). Inversions of teleseismic and strong motion records indicate the 3 November M7.9 event initiated by thrusting, followed by an eastward propagating unilateral rupture (Kikuchi and Yaminaka, 2002; Eberhart-Phillips et al., 2003). This unilateral rupture resulted in extreme directivity of seismic energy southeast of the rupture (Eberhart-Phillips et al., 2003; Hanson and Ratchkovski, this volume), and produced earthquake-related effects from Pennsylvania to Louisiana to Washington state. The westernmost surface rupture occurred on a previously unrecognized thrust fault named for the Susitna Glacier (Fig. 2). The broad arc of this initial rupture extends about 40 km along the southern flank of the Alaska Range. The convoluted surface trace is about 48 km long. The eastern end of the Susitna Glacier fault appears to connect with the Denali fault beneath the Susitna Glacier. On parts of the Susitna Glacier the surface rupture paralleled arcuate medial moraines, which indicates the glacier ice at least locally influenced the fault trace. Scarps seen on air photos suggest one or two previous Holocene events, but the westward extent of the Susitna Glacier fault beyond the 2002 rupture is unknown.

The principal rupture accompanying the 2002 earthquake is a 218-km break that reoccupied older fault scarps along the Denali fault. The western terminus of this rupture is about 15 km east of the epicenter and 10 km west of the intersection of the Denali and Susitna Glacier faults (Fig. 2). There was one 6.4-km-long WNW-striking splay that ruptured along the south side of the fault near Gillett Pass. Fault rupture through a glacier was reported in only one other earthquake - the1958 Fairweather fault earthquake, Alaska, where a 2 m dextral offset occurred on the Grand Plateau Glacier (Plafker et al., 1978).

At the eastern limit of rupture on the Denali fault, surface faulting stepped 14southeastward onto the Totschunda fault across a complex, 14-km-long transfer zone. The Denali fault did not break east of this intersection. There is, however, geomorphic expression of late Quaternary faulting farther southeast along the Denali fault (Clague, 1979). The transfer zone is characterized by a series of right-stepping fault segments, which are connected by north-striking east-side-up normal faults with displacements as large as 2.7 m, and a 7.9-km-long splay off the main trace of the Totschunda fault. The Totschunda surface ruptures extended a total of 76 km southeastward along the fault , mostly in a narrow zone of dextral offset. The rupture comprised the 14-km long transition zone, 53 km along the main

Totschunda Creek segment of the fault, 8 km along the Cooper Creek segment (Richter, 1975), and two areas without surface rupture, 2-km and 4-km long, which link the fault segments (Fig. 2).

The width of the zone of deformation along the strike-slip rupture was typically very narrow—no more than a few meters wide--where the fault trace was 'on land' (i.e. not through glacier ice) (Fig. 3D, 3E). Locally, where there were en echelon surface breaks, the zone of deformation was tens of meters wide. The zone of deformation reached approximately 100-m wide at the two locations where the fault displaced roads. These locations were along the Richardson Highway (and the TAPS) and the Tok Cutoff Highway. Both of these transportation corridors are in valleys with thick saturated Quaternary fill. Despite the wide zone of deformation in both places, most deformation was concentrated in a much narrower zone immediately adjacent to the fault trace, with only minor deflection of the roadbed observed more than 10 m from the fault trace. Along the Richardson Highway, the width of the concentrated zone of deformation was about 4 m, along the Tok Cutoff Highway, the width of the zone was about 20 m.

The fault trace varied from narrow to wide where the fault ruptured through glacier ice. For example, near the toe of the Canwell Glacier the fault trace was very linear and crossed crevasses with no deflection (Fig. 3G). On other glaciers, fault strands parallelled medial moraines (Fig. 3H), indicating the glacier ice influenced the surface trace. Complex fracture patterns cut across the ice fabric and connected multiple fault strands in some places. Thus, the glacier-ice fault traces did not always faithfully record the surface trace as well as off ice localities.

We examined the fault trace and measured offset features in November 2002 immediately after the earthquake, and also in July 2003. Along the fault, we observed numerous types of dextrally offset features. These included stream channels, channel banks, channel levees, channel thalwegs, tree roots, game trails, split cobbles, avalanche chute margins, glacier crevasses, and matching faces in glacial ice. We observed extensional and contractional stepovers, en echelon fissures, and Riedel shears in snow and glacier ice. We also found liquefaction of unconsolidated sediment near the fault trace in valley bottoms (see also Kayan et al., this volume).

The distribution of measured surface slip, both lateral and vertical, is shown on Figure 4. Uncertainties in slip measurements reflect uncertainties in piercing points and difficulties in projecting irregular offset features across the rupture zones. For the lateral offsets, we

characterized the slip distribution by enclosing the measurements within an envelope defined by the highest values. The overall distribution of slip along the Denali fault is asymmetric with higher slip to the east, and lower slip on the Totschunda fault (Fig. 4A). Right-lateral offset on the Denali fault dominates the slip distribution, with an average value of 4.9 m, and a maximum of 8.8 m 190 km east of the epicenter. The offset drops to zero abruptly at both ends. Offsets along the Totschunda fault are modest, by comparison. The average dextral offset is 1.7 m and the maximum is 3.1 m. Vertical slip on the Denali fault averaged 15% of the horizontal, and was dominantly north-side-up from the Totschunda fault to the intersection with the Susitna Glacier fault (Figure 4).

Large vertical slip along the Denali and Totschunda ruptures occurred where there were large horizontal offsets (Fig. 4B). The sense of vertical slip from measurements taken on glaciers is much more scattered than those taken off on land. Because ruptures through the glaciers commonly were diffuse and complex, we suggest that the vertical slip data from off-glacier sites is more reliable. Thus, looking only at the 'land' sites, the Denali fault has dominantly north-side-up slip from the Richardson Highway region to the Totschunda transition. Only the westernmost 'land' sites are south-side up. The vertical component of slip on Totschunda fault is a mixture of northeast and southwest-side up.

Thrusting on the Susitna Glacier fault raised the north side relative to the south. Scarp heights were typically 1 to 3-m high, with a maximum of 4.3-m (Craw et al., 2003). Two direct observations of fault dip were 10˚ and 25˚. Steeper fault dips of 48-75° were observed in glacier ice, but this was subparallel to, and probably influenced by, the ice fabric. Craw et al. (2003) estimate the dip slip, based on the near-surface dips and the scarp heights, to be 3-6 m. Lu et al. (2003) modeled the Susitna Glacier fault from Radarsat-derived interferograms. Their best-fit strike, dip, and rake were 251°, 40°, and 88°, respectively. First-motion analysis by the Alaska Earthquake Information Center (AEIC) gave an orientation of strike, dip, and rake of 262°, 48°, and 115°, and Kikuchi and Yamanaka (2002) obtained a strike, dip and rake of 227°, 40°, 99° from waveform inversion. The strike of the surface trace of the Susitna Glacier fault (249°) is closest to the interferogram modeling. The surface dip is shallower than that indicated by the teleseismic and interferometric models. Lu et al.'s (2003) best-fit uniform-slip model has 7 m of slip on the Susitna Glacier fault between 1.0 and 10.1 km depth, and a length of the fault zone of 20 km. This fault length is substantially shorter than the 40 km surface trace of the fault, and the slip value is significantly more than the 3-6 m derived from the typical scarp height and shallowest dips.

INTERPRETATION OF SLIP DISTRIBUTION

The slip distribution is critical data for a complete understanding of an earthquake. It provides direct observations of the source parameters for the earthquake and is not dependent upon the location, quality, and density of seismic instruments surrounding the rupture. Large-wavelength changes in surface slip values provide a physical basis for understanding the location and magnitude of seismologically interpreted sub-events.

The seismic moments calculated from teleseismic waveforms (M7.9, NEIC) agree well with the moment calculated from the average surface slip (M7.8). This calculation assumes an average of 4.9 m of right-slip on the Denali fault, 1.7 m of right slip on the Totschunda fault, and of 5 m of dip slip on a 30 km long part of the Susitna Glacier fault. The calculation also uses a depth of 11 km for the base of crustal seismicity, which is the base of well-defined aftershocks on the Denali fault. The average slip would have to be increased from 4.9 to 7.0 m on the Denali fault to yield a M7.9 earthquake.

There is some correlation between the source parameters of the earthquake from strong motion and GPS data and from the fault trace and slip distribution. In Eberhart-Phillips et al. (2003), the correlation appears remarkably good between the GPS, strong motion, and slip distribution data. Subsequent modelling of the strong motion (Frankel et al., 2003) and GPS (Hreinsdottir et al., 2003) data sets results in similar broad correlation with the slip distribution. However, in detail, our slip distribution does not correlate as well with the GPS and strong motion data. This relationship suggests either surface slip does not reflect slip at depth, or the models are not sufficiently refined. Nonetheless, all the models show large slip or moment release at the eastern end of the Denali fault, where the lateral surface slip averages 7.2 m between 160-210 km east of the epicenter.

Although there was not nearly as good an appreciation of how slip can vary along the length of fault ruptures, Woodward-Lundgren Associates (1974) made a remarkably good estimate of the magnitude of slip in a future Denali fault rupture. The TAPS was designed to accommodate 6.1 m right-lateral slip and 1.5 m vertical slip. Post-earthquake surveys indicate a total of 5.8 m of dextral slip across the fault zone (M. Metz, personal comm., 2003). The preconstruction geotechnical surveys had difficulty locating the fault trace in the vicinity of the pipeline, because the fault scarp is poorly expressed in the area (Woodward Lundgren Associates, 1974), and thus the pipeline was built with a 1-km wide zone built to

accommodate surface offset. The 2002 surface rupture was at the southernmost end of the special fault crossing zone. The accuracy of this forecast of the location and magnitude of slip demonstrates the importance and value of earthquake science in engineering design and risk mitigation.

Table 1. Summary of rupture parameters associated with each earthquake

FAULT	EARTHQUAKE	YEAR	Mw	LENGTH (km)	Dmax (m)	Davg (m)	COMPLEXITY	REFERENCE
San Andreas fault, California	San Francisco	1857	7.9	300	9.5	5.5	No known associated rupture	Sieh, 1978
Bulnay fault, Mongolia	Bulnay fault	1905	8.0	375	11	8	Thrust faulting	Baljinnyam et al (1993); Schwartz et al (1999)
San Andreas fault, California	San Francisco	1906	7.8	470	6.4	5	No known associated rupture	Lawson (1908)
Haiyuan fault, China	Haiyuan fault	1920	7.9	240	10	--	No known associated rupture	Deng et al (1986)
North Anatolian fault, Turkey	Erzincan	1939	7.9	327	7.6	4.7	No known associated rupture	Barka (1996)
Bogd fault, Mongolia	Gobi Altay	1957	7.8	260	8	4.5	Thrust faulting	Florensov and Solenenko (1965); Baljinnyam et. al.(1993)
Kunlun fault, Tibet	Kunlunshan	2001	7.8	350	7.6	4	Multiple strands in a wide zone	Xu et al (2002)
Denali fault, Alaska	Denali fault	2002	7.9	300(strike-slip); 340 (total)	8.8	4.9	Thrust faulting	Eberhardt-Phillips etal (2002); this paper

COMPARISON TO OTHER LARGE STRIKE-SLIP RUPTURES

The M7.9 Denali fault earthquake ranks among the largest strike-slip ruptures during the past century and a half. Its rupture length, average and maximum slip, and magnitude are comparable with only a handful of earthquakes that have occurred in the shallow crust around the world since 1850 (Table 1). These earthquakes include:1857 central San Andreas, California; 1905 Bulnay, Mongolia; 1906 San Francisco, California; 1922 Haiyuan, China; 1939 Erzincan, Turkey; 1957 Gobi Altay, Mongolia; and 2001 Kunlun, Tibet. The rupture parameters associated with each of these earthquakes are summarized in Table 1. Long strike-slip faults, such as these, have a well-defined surface expression that developed from repeated large-slip earthquakes, and typically produce relatively narrow and simple surface

fault traces. For some of these historical earthquakes, coseismic rupture also occurred on associated faults, which are commonly large thrust faults. This is the case for the 1905 Bulnay (Teregtiyn thrust) and 1957 Gobi-Altay (Toromhohn, Gurvan-Bulag,and Dalam-Turu thrusts), Mongolia earthquakes as well as the 2002 Denali (Susitna Glacier thrust) event. This phenomenon should be considered when evaluating hazards from other large strike-slip faults. Although it is less well documented for the older surface ruptures (Table 1), slip is also variable along their length.

Wells and Coppersmith (1994) examined empirical relationships between earthquake magnitude, rupture length, rupture width, rupture area, and surface displacement. Their regressions are commonly used in seismic hazard analysis to estimate the expected size of future earthquakes from observations or inferences of fault parameters. The best correlation between the fault parameters is the relationship between rupture area (fault length x fault width) and moment magnitude (M). However, the relationship increasingly underestimates M for larger rupture areas (Fig. 5). Hanks and Bakun (2002) updated the Wells and Coppersmith (1994) database with additional information about large strike-slip earthquakes (including those listed in Table 1, minus the Denali fault earthquake), and concluded that two lines better fit a regression of the data. The Denali fault earthquake provides another data point for assessing these relations (Fig. 5). We assume a width of the Denali fault zone as 12 km, based on the depth of aftershocks (Ratchkovski and Hansen, 2003) and a fault length of 340 km. This probably slightly underestimates the fault area associated with the Susitna Glacier fault, but it does not change the position of the datapoint on the magnitude versus area plot perceptibly (Fig. 5). The Denali fault earthquake plots in the same field of data as other earthquakes with a similar magnitude and rupture area, near the Hanks and Bakun (2002) regression line, and above the Wells and Coppersmith (1994) regression line, which would have yielded a M of 7.6.

The 2002 Denali fault earthquake can help us understand the effects expected in future large strike-slip earthquakes. For example, the southern section of the San Andreas fault between San Bernardino and the Salton Sea (Coachella Valley segment) and the Denali fault west of the 2002 epicenter have lengths of several hundred kilometers and large single-event paleoearthquake offsets. Both of these faults are expected to produce earthquakes with a magnitude, rupture length, and offset similar to the 2001 Denali event. The unilateral rupture of the 2002 Denali fault earthquake brings up an additional issue of the directivity of the rupture. Future engineering studies should consider directivity effects of large earthquakes.

CONCLUDING REMARKS

The Denali fault earthquake surface rupture reoccupied previous scarps along the Denali and Totschunda faults. The coincident surface ruptures confirm the notion that the location, and possibly the offset in future earthquakes can be learned from past ones. Moreover, historical records of slip along surface ruptures provide direct observations that relate to the amount of energy released along a fault. The slip distribution along the Denali and Totschunda faults from the November 2002 **M**7.9 earthquake is an important data set for considering surface offset of large strike-slip faults around the world. Geologists and engineers should consider variable slip along the strike of the rupture, potential directivity effects, as well as the structural complexities of the rupture.

ACKNOWLEDGEMENTS

REFERENCES CITED

Baljinnyam, I., Bayasgalan, A., Borisov, B.A., Cisternas, A., Dem'yanovich, M.G., Ganbaatar, L., Kochetkov, V.M, Kurushin, R.A., Molnar, P., Philip, H., and Vaschilov, Yu. Ya., 1993, *Ruptures of major earthquakes and active deformation in Mongolia and it's surroundings:* Geological Society of America Memoir 181, 62 pp.

Barka, A.A., 1996, *Slip distribution along the North Anatolian fault associated with large earthquakes of the period 1939 to 1967*, Seismological Society of America Bulletin, v. 86, pp. 1238-125.

Clague, J.J., 1979, *The Denali fault system in southwest Yukon Territory – A geologic hazard?*: Current Research, Part 1, Geological Survey of Canada Paper 79-1A, p. 169-178.

Craw, P.A., Crone, A.J., Haeussler, P.J., Personius, S.F., and Staft, L.A., 2003, *The Susitna Glacier thrust fault-characteristics of ruptures that initiated the Denali fault earthquake (abstract)*: Eos Trans. AGU, S11B, 84(46) Fall Meeting Suppliment, Abstract S11B-01

Deng, Q., Chen, S., Song, F.M., Zhu, S., Wang, Y., Zhang, W., Burchfiel, B.C., Molnar, P., Royden, L., And Zhang, P., 1986, *Variations in the geometry and amount of slip on the Haiyuan fault zone, China and the surface rupture of the 1920 Haiyuan earthquake*: Earthquake Source Mechanics, Geophysical Monograph, v. 3, p. 169-182.

Eberhart-Phillips, D., Haeussler, P.J., and Freymueller, J.T., et al., 2003, *The 2002 Denali fault earthquake, Alaska: A large magnitude slip-partitioned event*: Science, v. 300, p. 1113-1118.

Florensov, N.A., and Solonenko, 1965, *The Gobi-Altay earthquake (in Russian)*: Moscow, Akademiya Nauk USSR, (English translation by Israel Program for Scientific Translations) Washington, D.C., U.S. Department of Commerce, 391 p.

Frankel, A., 2003, *Source process of the M7.9 Denali fault, Alaska, earthquake: sub-events, directivity, and scaling of high-frequency ground motion*: Eos Trans. AGU, 84(46) Fall Meeting Suppliment, Abstract S11H-03.

Grantz, A., 1966, Strike slip faults in Alaska: U.S. Geological Survey Open-File Report 267.

Haeussler, Peter H., Bruhn, Ronald L., and Pratt, Thomas L., 2000, *Potential seismic hazards and tectonics of upper Cook Inlet Basin, Alaska, based on analysis of Pliocene and younger deformation*: Geological Society of America Bulletin, v. 112, p. 1414-1429.

Haeussler , Peter J., Schwartz, David P., Dawson, T.E., Stenner, H.D., Lienkaemper, J.J., Cinti, F., Montone, P., Sherrod, B., Crone, A.J., Personius, S., submitted 2004, *Surface Rupture and Slip Distribution of the 3 November 2002 M7.9 Denali fault earthquake, Alaska*: Bulletin of the Seismological Society of America.

Hanks, T.C., and Bakun, W.H., 2002, *A bilinear source-scaling model for **M**-log A observations of continental earthquakes*: Bulletin of the Seismological Society of America, v. 92, p. 1841-1846.

Hanson, R.A., and Ratchkovski, N.A., 2004, *Seismological aspects of the Mw 7.9 2002 Denali fault, Alaska earthquake*: Earthquake Spectra, this issue.

Hreinsdottir, S., Freymueller, J.T., Fletcher, H.J., Larson, C.F., and Burgman, R., 2003, *Coseismic slip distribution of the 2002 Mw7.9 Denali fault earthquake, Alaska, determined from GPS measurements*: Geophysical Research Letters v. 30, 1670, doi:10.1029/2003GL017447.

Kayen, R., Thompson, E., Minasian, D., Collins, B., Moss, E.R.S., Sitar, N., Carver, G., 2004, *Geotechnical reconnaissance of the November 3, 2002, M7.9 Denali fault, Alaska, earthquake*: Earthquake Spectra, this volume.

Kikuchi, M., and Yamanaka, Y., 2002, *Source rupture processes of the central Alaska earthquake of Nov. 3, 2002, inferred from teleseismic body waves (+the 10/23 M6.7 event)*, EIC seismological note – No. 129, Earthquake Research Institute (ERI), Univ. Tokyo, Tokyo. http://wwweic.eri.u-tokyo.ac.jp/EIC/EIC_News/021103AL-e.html

Lahr, J.C., and Plafker, G., 1980, *Holocene Pacific-North American plate interaction in southern Alaska; implications for the Yakataga seismic gap*: Geology, v. 8, p. 483-486.

Lawson, A.C., chairman,1908, *The California earthquake of April 18, 1906*: Report of the State Earthquake Investigation Committee (volume 1), Carnegie Institution of Washington, Pub. 87

Lu, Z., Wright, T., and Wicks, C., 2003, *Deformation of the 2002 Denali fault earthquakes, mapped by Radarsat-1 interferometry*: Eos, v. 84, p. 425-431.

Plafker, George, Hudson, T., Bruns, T.R., and Rubin, M., 1978, *Late Quaternary offsets along the Fairweather fault and crustal plate interactions in southern Alaska*: Canadian Journal of Earth Sciences, v. 15, p. 805-816.

Plafker, G., Hudson, T., and Richter, D.H., 1977, *Preliminary observations on late Cenozoic displacements along the Totschunda and Denali fault systems*, U.S. Geological Survey Circular 751-B, B67

Plafker, George, 1969, *Tectonics of the March 27, 1964 Alaska earthquake*: U.S. Geological Survey Professional Paper, P-543I, p. I1-I74.

Plafker, G., Moore, J.C., and Winkler, G.R. 1994. *Geology of the Southern Alaska Margin, In: The Geology of Alaska, Decade of North American Geology*, v. G-1, edited by Plafker, G.,and Berg, H.C., Geological Society of America, Boulder, Colorado, p. 989-1022.

Ratchkovski, N.A., and Hansen, R.A., 2003, *The 2002 Denali fault, Alaska, earthquake sequence recorded on the regional network: earthquake locations, magnitudes, and focal mechanisms*: Eos Transactions AGU, v. 84, Fall Meeting Supplement, Abstract S12A-0363.

Richter, D., and Matson, N., 1971, *Quaternary faulting in the eastern Alaska Range*: Geological Society of America Bulletin, v. 82, p.1529-1539.

Richter, D. H., 1975, *Reconnaissance geologic map of the Nabesna B-3 quadrangle, Alaska*: U. S. Geological Survey Miscellaneous Investigations Series Map I-904.

Schwartz, D. P., Hecker, S., Ponti, D. J., Bayasgalan, A.,. Lund, W. R., Stenner, H. D., and Enkbaatar, D., 1999, *Paleoseismic reconnaissance along the Great 1905 Bulnay, Mongolia surface rupture [*abs]: Seismological Research Letters, in SSA-99 94th annual meeting; meeting abstracts. v. 70, no. 2, p. 235.

Sieh, K., 1978, *Slip along the San Andreas fault associated with the great 1857 earthquake*: Seismological Society of America Bulletin, v. 68, p. 1421-1428.

St. Amand, P., 1957, *Geological and geophysical synthesis of the tectonics of portions of British Columbia, the Yukon Territory, and Alaska*: Geological Society of America Bulletin, v. 68, p. 1343-1370.

Wells, D.L., and Coppersmith, K.J., 1994, *New empirical relationships among magnitude, rupture length, rupture width, rupture area, and surface displacement*: Bulletin of the Seismological Society of America, v. 84, p. 974-1002.

Woodward-Lundgren Associates, 1974, *Summary Report, Basis for pipeline design for active-fault crossings for the trans-Alaska pipeline system, Appendix A-3,* variously paginated.

Wright, T.J., Lu, Z., and Wicks, C., 2003, *Source model for the Mw 6.7, 23 October 2002, Nenana Mountain earthquake (Alaska)* from InSAR: Geophysical Research Letters, v. 30, 18, 1974, doi: 10.1029/2003GL018014.

Xu, X., Chen, W., Ma, W., Yu, G., and Chen, G., 2002, *Surface Rupture of the Kunlunshan Earthquake (Ms 8.1), Northern Tibetan Plateau, China* Seismological Research Letters, v. 73, p. 884-892.

Figure 1. Tectonic setting of the Denali fault in southern Alaska. The Yakutat terrane is colliding with the southern Alaska margin, causing faulting into interior Alaska (Lahr and Plafker, 1980). Arrows with bars behind them show the relative motion between the Pacific plate and North America and the Yakutat terrane and North America. Open arrows show the motion of the Wrangell Block with respect to North America.

Figure 2. Rupture map of the 2002 Denali fault earthquake. Epicenter of 3 November 2002 mainshock is shown by the star on the left. TCS, Totschunda Creek strand of the Totschunda fault; CCS, Cooper Creek strand of the Totschunda fault.
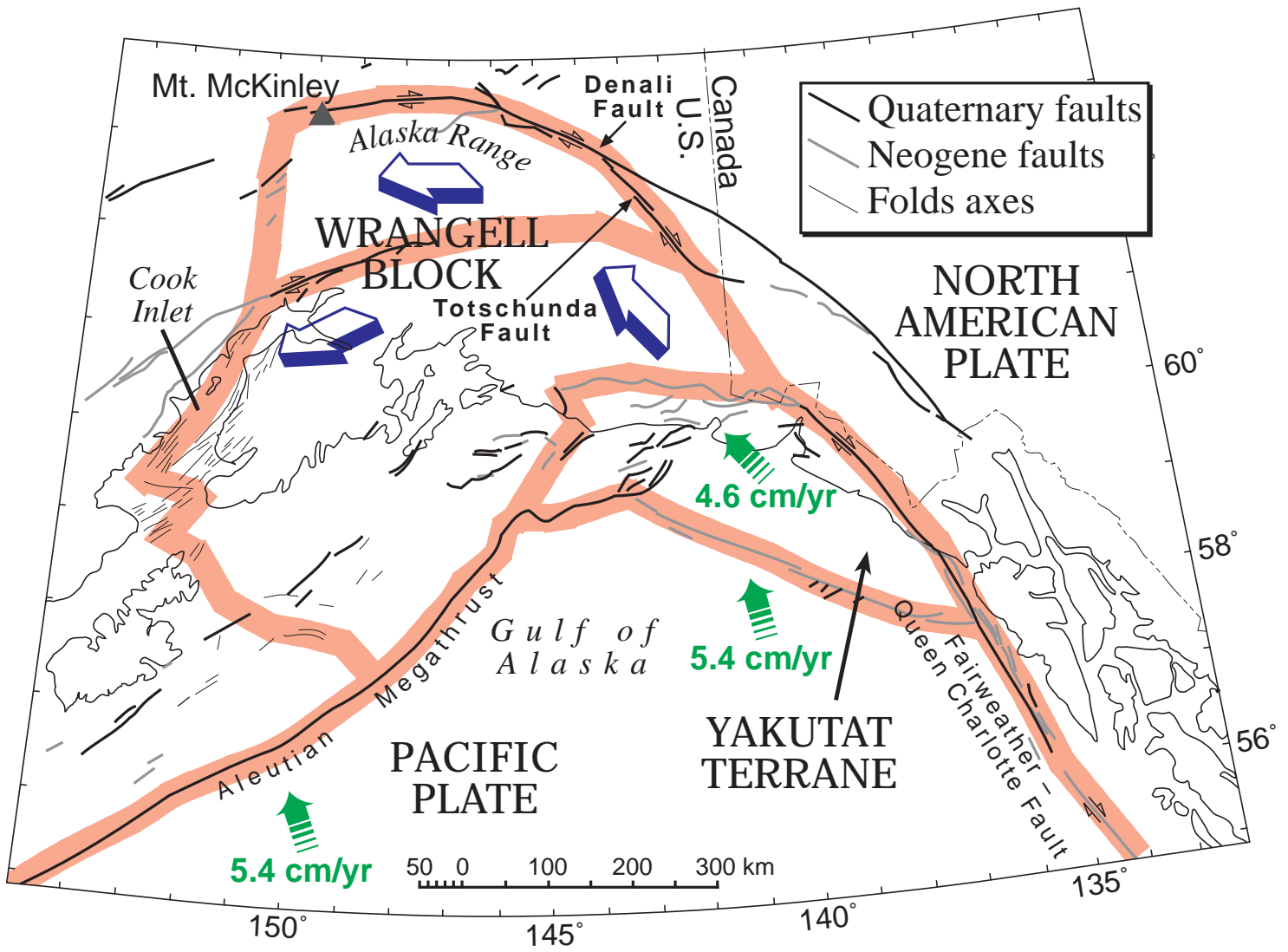
Figure 3. Photographs of the surface ruptures. All photographs taken in November of 2002, except for (E), which were taken in July of 2003. A) Susitna Glacier thrust fault on the Susitna Glacier. The fault was discovered near here. View is toward the southwest. B) Susitna Glacier fault, southwest of the Susitna Glacier. View is toward the northeast. Scarp is 1.5-2 m tall. C) Susitna Glacier fault scarp. Note the small birch tree, behind the stadia rod, which was overthrust by the fault. Also, note the extensional cracks in the snowpack, caused by the tip of the thrust rolling over. Marked gradations on stadia rod are decimeters. D) Denali fault trace. Note the narrow mole track, linear trace, and the Riedel shears in the snow pack indicating right-lateral shear. The lack of cracks more than a few meters from the fault trace indicates little deformation occurred away from the main rupture. View is toward the east and Gillett Pass. The fault takes a step to the right (north) at the pass. E) Denali fault trace in the Slate Creek area. Note linear fault trace and lack of defomation off the fault trace. View is toward the west. F) Totschunda fault trace, near its southern extent. Like the Denali fault, the trace is straight with little evidence of shearing away from the surface rupture. View is toward the southeast. G) Denali fault trace on the Canwell glacier. The fault trace cuts across crevasses in the center of the photo, and shows how the fault trace through glacier ice can be simple, narrow, and apparently not influenced by glacial ice fabric. View is toward the east. H) Denali fault trace showing a complex fault trace on glacial ice. Thin black dashed lines parallel surface breaks. Note how the fault trace parallels the medial moraines, and the complex pattern between multiple fault strands. This indicates the glacial ice fabric influences the surface trace.
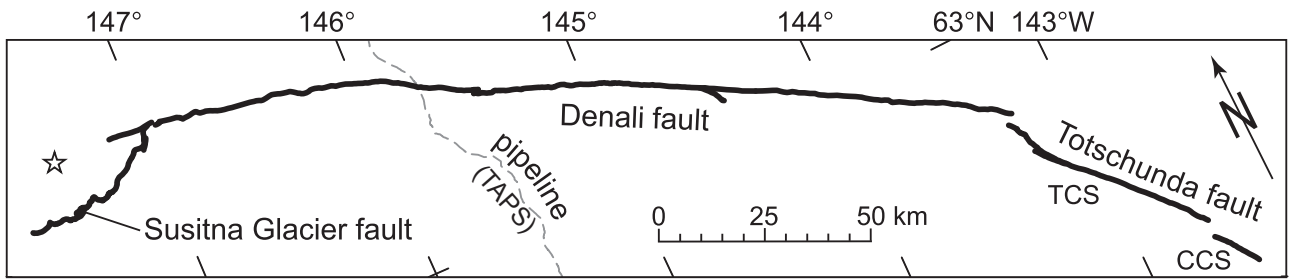
Figure 4. Slip distribution along the Denali and Totschunda faults. A) Horizonta slipl. A line that runs through the largest measured values is shown, and labeled as "Envelope of Maximum Slip." B)

Vertical slip. Data from Eberhart-Phillips et al. (2003) and Haeussler et al. (in prep). For preliminary Susitna Glacier fault data, not shown here, see Craw et al. (2003).

Figure 5. Plot of moment magnitude (**M**) versus log of rupture area (A) of strike-slip earthquakes, modified from Hanks and Bakun (2002). Denali fault earthquake is denoted by grey star. Regression line of Wells and Coppersmith (1994) is shown by dashed grey line labeled (WC94). This line underestimates the magnitude of earthquakes larger than magnitude 7. Regression lines of Hanks and Bakun (2002) shown by solid grey lines labeled (HB02).

Table 1. Comparison of surface rupture parameters of large strike-slip earthquakes. Moment magnitude (Mw) is either instrumentally determined or estimated from fault parameters. Length is the measured strike-slip surface rupture; Dmax is the maximum observed surface offset; Davg is the average slip for the entire rupture based on surface slip distribution; complexity is the occurrence of coseismic surface rupture on associated faults.

Quaternary faults
Neogene faults
Folds axes

Mt. McKinley

Denali Fault

Canada U.S.

Alaska Range

WRANGELL BLOCK

NORTH AMERICAN PLATE

60°

Cook Inlet

Totschunda Fault

Aleutian Megathrust

Gulf of Alaska

4.6 cm/yr

58°

5.4 cm/yr

YAKUTAT TERRANE

Fairweather – Queen Charlotte Fault

56°

PACIFIC PLATE

5.4 cm/yr

50 0   100   200   300 km

135°

150°   145°   140°

147°   146°   145°   144°   63°N 143°W

Denali fault

Totschunda fault

☆

Susitna Glacier fault

pipeline
(TAPS)

0   25   50 km

TCS

CCS

N

Figure 3.

A) Horizontal slip measurements along the Denali Fault and Totschunda Fault plotted against distance from epicenter (km). Legend: July 2003 measurements (green), November 2002 measurements (orange), culled measurements (open circles). Labeled regions include Susitna - Black Rapids Glacier, Canwell - Gakona Glaciers, Chistochina Glacier, and Denali - Totschunda Step-Over. Location markers along the base axis: Epicenter, Augustana Creek, Pipeline, Richardson Hwy, Slate Creek, Slana River, Gillett Pass, Mentasta, Tok Cutoff, Little Tok River, Nabesna River, Blue Lake.

B) Vertical Displacement (cm) plotted against Distance from Epicenter (km). Legend: North Side Up (green triangles), South Side Up (orange circles).

M = 4/3 log A + 3.07, for A 537 km
(HB02)

M = log A + 3.07, for A ≤ 537 km
(HB02)

M = log A + 4.03
(WC94)